COMPUTATIONAL MECHANICS 2019
35th conference with international participation
Srní
November 4 - 6, 2019

The influence of penalization inlet boundary condition on the stability boundary

J. Valášek[a], P. Sváček[a], J. Horáček[b]

[a] Faculty of Mechanical Engineering, Czech Technical University in Prague, Karlovo nám. 13, Praha 2, 121 35
[b] Institute of Thermomechanics, Czech Academy of Sciences, Dolejškova 5, Praha 8, 182 00

The flow-induced vibrations of human vocal folds (VFs) are interesting and complex phenomenon with number of possible practical applications, see e.g. [2, 3]. Mathematically it represents the fluid-structure interaction (FSI) problem which in this specific case poses many difficulties for numerical realization. One of the major difficulty is need to consider the flow domain time evolution especially during the closing phase, see [5], followed by the question of a suitable inlet boundary condition, see [4] etc. We present here the two-dimensional FSI model, see Fig. 1, where linear elastic problem is coupled to the incompressible Navier-Stokes equations in the arbitrary Lagrangian-Eulerian (ALE) form. The special attention is paid to the flow inlet boundary conditions (BCs), where the penalization boundary condition is introduced as a promising alternative to the usually used Dirichlet boundary condition or to the prescribed pressure drop between inlet and outlet.

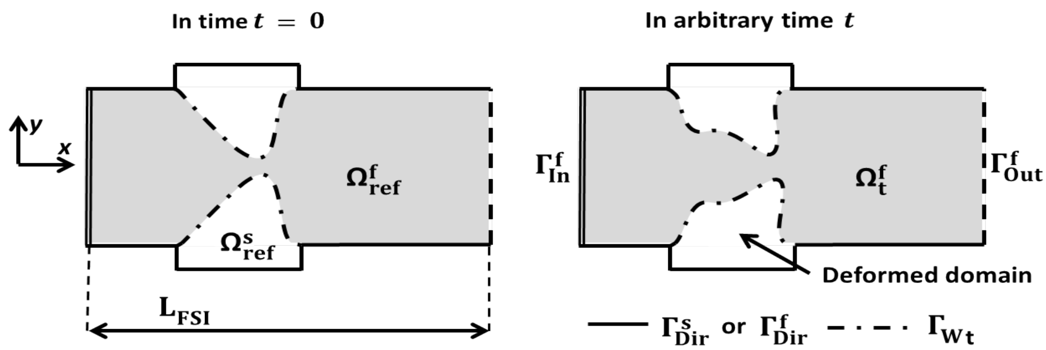

Fig. 1. The scheme of FSI domain composed of fluid domain Ω^f_t and the elastic body domain Ω^s

Structure. The motion of structure with density ρ^s is given by partial differential equations

$$\rho^s \frac{\partial^2 u_i}{\partial t^2} - \frac{\partial \tau^s_{ij}}{\partial x_j} = 0 \qquad \text{in } \Omega^s \times (0,T), \tag{1}$$

where $\mathbf{u}(x,t) = (u_1, u_2)$ is sought displacement and τ^s_{ij} are the components of the Cauchy stress tensor [1]. The small displacements are assumed and the elastic body is modelled as isotropic.

Fluid flow. In order to incorporate the effects of the fluid computational domain, the ALE method is used. The motion of the viscous incompressible fluid in a time dependent domain Ω^f_t is modelled by the Navier-Stokes equations written in the ALE form

$$\frac{D^A\mathbf{v}}{Dt} + ((\mathbf{v} - \mathbf{w}_D)\cdot\nabla)\mathbf{v} - \nu^f\Delta\mathbf{v} + \nabla p = \mathbf{0}, \quad \operatorname{div}\mathbf{v} = 0 \quad \text{in } \Omega^f_t, \tag{2}$$

where $\mathbf{v}(x,t)$ denotes the fluid velocity, p is the kinematic pressure and ν^f is the kinematic fluid viscosity, further the term $\frac{D^A}{Dt}$ denotes so called ALE derivative and the term $\mathbf{w}_D$ is domain deformation velocity, see e.g. [1].

The system of equations (2) is equipped with the zero initial condition and appropriate BC, see [6]. Especially, on the inlet $\Gamma^f_{\rm In}$ the three different inlet BC are considered

$$\begin{aligned}
&\text{a)} && \mathbf{v}(x,t) = \mathbf{v}_{\rm Dir}(x,t) && \text{for } x \in \Gamma^f_{\rm In},\\
&\text{b)} && (p(x,t) - p_{\rm in})\vec{n}^f - \nu^f \frac{\partial \mathbf{v}}{\partial \vec{n}^f}(x,t) = -\frac{1}{2}\mathbf{v}(\mathbf{v}\cdot\vec{n}^f)^- && \text{for } x \in \Gamma^f_{\rm In},\\
&\text{c)} && p(x,t)\vec{n}^f - \nu^f \frac{\partial \mathbf{v}}{\partial \vec{n}^f}(x,t) = -\frac{1}{2}\mathbf{v}(\mathbf{v}\cdot\vec{n}^f)^- + \frac{1}{\epsilon}(\mathbf{v} - \mathbf{v}_{\rm Dir}) && \text{for } x \in \Gamma^f_{\rm In},
\end{aligned} \tag{3}$$

where the vector $\mathbf{n}^f = (n^f_j)$ denotes the outward unit normal to the boundary $\partial\Omega^f$ and $\alpha^+ = \max\{0,\alpha\}$, $\alpha^- = \min\{0,\alpha\}$, see [6]. The condition (3 c) is weakly imposed Dirichlet boundary condition, which fulfilment is enforced with the aid of penalization coefficient ϵ.

Numerical model. The FSI problem given by Eqs. (1) and (2) together with appropriate initial and boundary conditions are discretized in space by the finite element method and in time by the Newmark method. The partitioned approach with strong coupling is chosen. Especially, the modified streamline-upwind/Petrov-Galerkin method is used for stabilization of flow solver. For implementation details, see [6].

Numerical results. Numerical results of flow-induced vibration of vocal folds (VFs) with the full channel configuration are presented. The VF geometry is based on articles [4] and [6]. The constant time step Δt is chosen as 2.5×10^{-5} s, the densities are set to $\rho^s = 1000\,\mathrm{kg/m^3}$ and $\rho^f = 1.185\,\mathrm{kg/m^3}$, the kinematic fluid viscosity is $\nu^f = 1.47 \times 10^{-5}\,\mathrm{m^2/s}$. The elastic parameters are chosen as follows: Young modulus $E^s = 8\,\mathrm{kPa}$ and Poisson ratio $\sigma = 0.4$.

Comparison of different inlet boundary conditions. The following four simulations with different inlet boundary conditions are compared, namely:

a) Case *VEL* with prescribed Dirichlet BC (3 a) with $\mathbf{v}_{\rm dir} = (2.1, 0.0)\,\mathrm{m/s}$,

b) Case *PEN-S* with penalization BC (3 c), where velocity $\mathbf{v}_{\rm dir}$ is imposed by $\epsilon = 10^{-5}$,

c) Case *PEN-W* with penalization BC (3 c), where velocity $\mathbf{v}_{\rm dir}$ is imposed by $\epsilon = 5 \times 10^{-4}$,

d) Case *PRES* with given pressure drop $\Delta p = p_{\rm in} - p_{ref} = 400\,\mathrm{Pa}$ in (3 b).

The inlet flow velocity and the pressure drop are displayed in Fig. 2. While the inlet velocity is for Dirichlet BC constant and for the prescribed pressure drop highly oscillating, in cases *PEN-S* and *PEN-W* we see the moderately oscillation behaviour of inlet velocity. The amplitude of oscillation increases with the higher values of penalization parameter ϵ ($\frac{1}{\epsilon}$ is decreasing).

The pressure drop in the case *PRES* is constant, see Fig. 2 (right), whereas in cases *VEL*, *PEN-S* and *PEN-W* it oscillates with exponentially increasing amplitude. This can be expected because the inlet velocity $\mathbf{v}_{\rm Dir}$ exceeds critical velocity of flutter instability $\mathbf{v}_{flutter}$. Then the VF oscillation amplitude gradually grows and the airflow pressure increases as the channel cross-section becomes smaller. The increase of pressure drop is most rapid for case *VEL*, the cases *PEN-S* and *PEN-W* are time delayed. The simulations in all four cases end by the fluid flow solver failure caused by too distorted fluid computational mesh near the top of the VFs.

The gap denoting the distance between vocal folds is plotted in Fig. 3. The gradually closing gap corresponds well with pressure drop behaviour in cases *VEL*, *PEN-S* and *PEN-W*. In the case *PRES* the VF oscillation develops despite constant pressure drop nevertheless the development of large VF oscillation took longer time. We found explanation in the fact, that prescribed Δp lays more closer to stability boundary contrary to given inlet velocity $\mathbf{v}_{\rm Dir}$, which substantially exceeds the stability boundary.

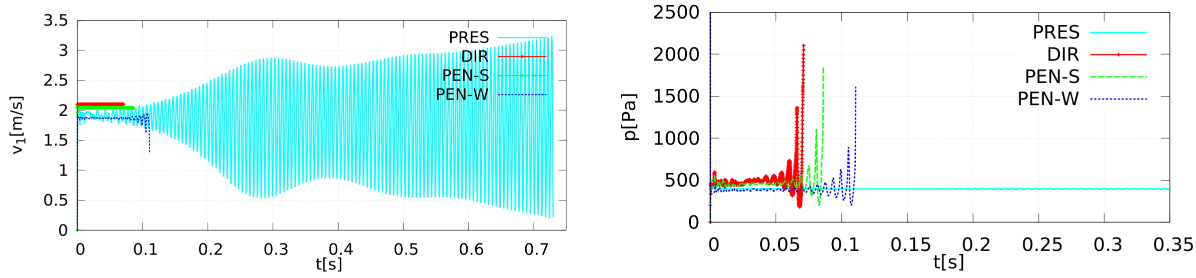

Fig. 2. The numerically simulated inlet airflow velocity and pressure difference between inlet and outlet of the channel are shown on the left and on the right, respectively. The simulation cases *VEL*, *PEN-S*, *PEN-W* and *PRES* are compared.

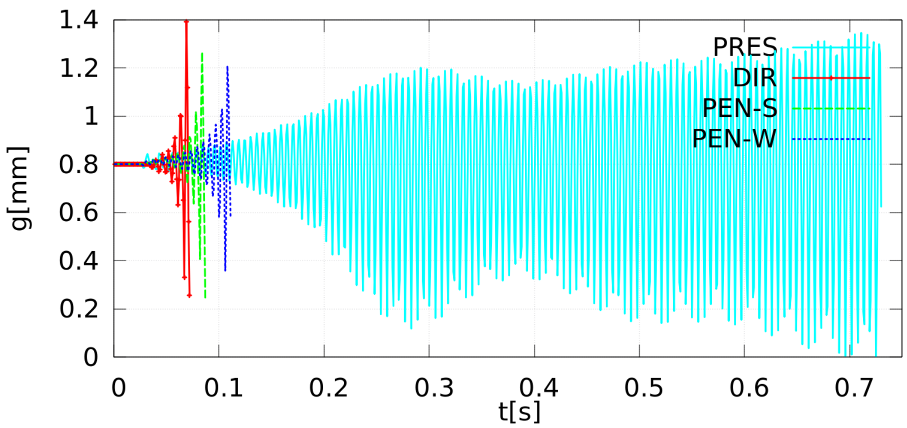

Fig. 3. Time development of the gap numerically simulated for cases *VEL*, *PEN-S*, *PEN-W* and *PRES* (The graph envelope is undulated due to too low sampling rate for saving the data for drawings.)

Comparison of simulations with hemi-larynx and full larynx configuration. The simulations with the full larynx geometry are compared with the hemi-larynx geometry as performed in [6], where the flow symmetry along x-axis is assumed in order to considerably reduce computational time. The numerical approximation of FSI problem for both configurations at one time instant are shown in Fig. 4.

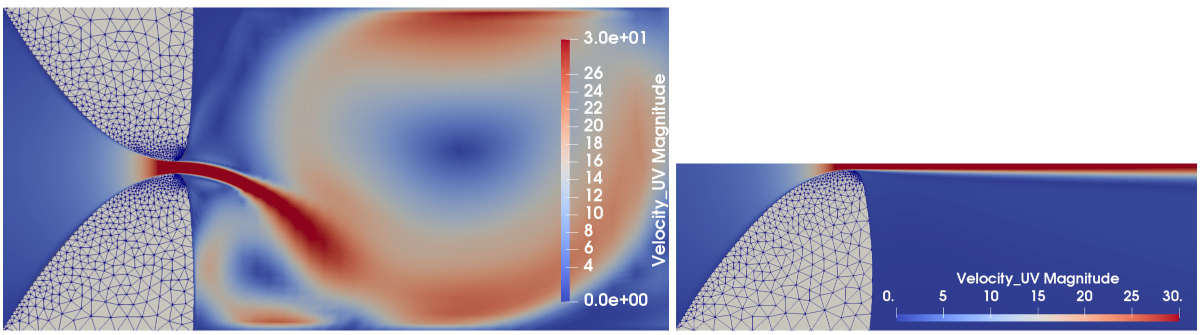

Fig. 4. The airflow velocity magnitude shown in similar time instant during closing phase of VF oscillation cycle. The simulation case *PEN-W* (full larynx configuration) is shown left, the simulation with hemi-larynx configuration is also computed with prescribed penalization BC (3 c) enforced with the aid of $\epsilon = 5 \times 10^4$.

Finally, the critical velocity of flutter instability $v_{flutter}$ is determined by the successively increasing the prescribed airflow inlet velocity until the unstable VF vibration regime occurs. Further, we studied the dependence of the determined critical velocity on the penalization parameter, see Fig. 5. The dependency of velocity $v_{flutter}$ on the parameter ϵ in the range $1 \times 10^{-10} < \epsilon < 5 \times 10^{4}$ is compared for both configurations, i.e., the geometry of full larynx and hemi-larynx. The both dependencies show the similar behaviour however exact values slightly differs. Nevertheless the computationally cheaper simulation of the hemi-larynx configuration can be used to estimate quite well the critical velocity of the full larynx configuration.

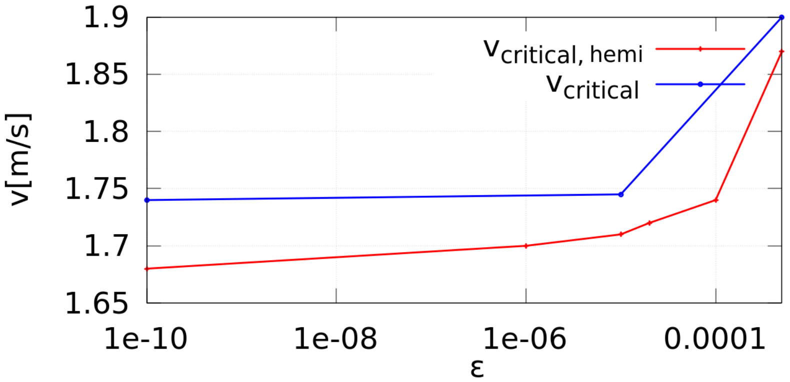

Fig. 5. The dependencies of critical velocity of flutter instability on the penalization parameter. The dependency of simulations with the full larynx configuration is plotted by blue curve, while the dependency of simulations with the hemi-larynx configuration is denoted as $v_{critical,hemi}$.

Acknowledgments

Authors are grateful for support provided by *Grant No. GA19-04477S* of Czech Science Foundation and by *Grant No. SGS19/154/OHK2/3T/12* of the CTU in Prague.

References

[1] Feistauer, M., Sváček, P., Horáček, J., Numerical simulation of fluid-structure interaction problems with applications to flow in vocal folds, In: T. Bodnár, G. P. Galdi, S. Nečasová (eds.), Fluid-structure interaction and biomedical applications, Birkhauser, 2014, pp. 312-393.

[2] Horáček, J., Radolf, V., Laukkanen, A. M., Experimental and computational modeling of the effects of voice therapy using tubes, Journal of Speech, Language, and Hearing Research 62 (7) (2019) 2227-2244.

[3] Mittal, R., Zheng, X., Bhardwaj, R., Seo, J. H., Xue, Q., Bielamowicz, S., Toward a simulation-based tool for the treatment of vocal fold paralysis, Frontiers in Physiology 2 (19) (2011) 1-15.

[4] Sváček, P., Horáček, J., Finite element approximation of flow induced vibrations of human vocal folds model: Effects of inflow boundary conditions and the length of subglottal and supraglottal channel on phonation onset, Applied Mathematics and Computation 319 (2018) 178-194.

[5] Sváček, P., Valášek, J., Mathematical modelling and numerical simulation of flow induced vibrations of vocal folds model with collisions, AIP Conference Proceedings 2116 (2019) No. 030003, doi: 10.1063/1.5113987.

[6] Valášek, J., Sváček, P., Horáček, J., On suitable inlet boundary conditions for fluid-structure interaction problems in a channel, Applications of Mathematics 64 (2) (2019) 225-251.